Unveiling the spectral transition of Aql X-1 from the hard to soft state

Ko Ono,[1] Kazuo Makishima,[2] Soki Sakurai,[1]
Zhongli Zhang,[3] Kazutaka Yamaoka[4,5] and Kazuhiro Nakazawa[1]

[1] Department of Physics, The University of Tokyo, 7-3-1 Hongo, Bunkyo-ku, Tokyo 113-0033, Japan
[2] MAXI Team, Global Research Cluster, The Institute of Physical and Chemical Research, 2-1 Hirosawa, Wako, Saitama 351-0198, Japan
[3] Shanghai Astronomical Observatory, Chinese Academy of Sciences, 200030 Shanghai, China
[4] Division of Particle and Astrophysical Science, Graduate School of Science, Nagoya University, Furo-cho, Chikusa-ku, Nagoya, Aichi 464-8602, Japan
[5] Institute for Space-Earth Environmental Research (ISEE), Nagoya University, Furo-cho, Chikusa-ku, Nagoya, Aichi 464-8601, Japan
E-mail(KO): ono@phys.s.u-tokyo.ac.jp

Abstract

The recurrent X-ray transient Aquila X-1 was observed with Suzaku on 2011 October 21 when the source is in a rising phase of an outburst. The unabsorbed 0.1–100 keV luminosity increased from 3.5×10^{37} erg s^{-1} to 5.1×10^{37} erg s^{-1}, and the 0.8–10 keV XIS count rate increased by a factor of ~ 3, while the 15–60 keV HXD-PIN count rate decreased to about one third. The spectrum showed a clear transition from the soft state to the hard state, changing in shape from a cutoff power-law like shape to a convex thermal one. Throughout the transition, the spectrum was successfully explained by a common model, consisting of a multi-color disk blackbody from a standard accretion disk and a blackbody emission from the neutron star surface Comptonized by a corona. The transition is characterized by continuous changes of the model parameters; the inner disk radius decreased from 31 km to 18 km, and the coronal temperature decreased from 10 keV to 3 keV accompanied by a shrink of the corona toward the neutron star surface. Furthermore, the fractional 0.1–100 keV luminosity carried by the disk emission increased from 21% to 56%.

Key words: accretion, neutron star, X-ray binary

1. Introduction

Some Neutron-Star (NS) Low-Mass X-ray Binaries (LMXB), consisting of weakly magnetized NSs and low-mass stars, are known to undergo outbursts. When the luminosity exceeds $\sim 4\%$ of the Eddington luminosity, the spectrum changes drastically from the hard state exhibiting a power-law like shape with a cutoff at > 10 keV to the soft state showing a convex thermal one (Asai et al. 2012). Thanks to broad-band Suzaku data, the spectra in the two states have been described in a unified way with three elements, multi-color disk (MCD) emission from an accretion disk, a blackbody (BB) emission from the NS surface, and a hot corona that Comptonizes the BB photons weakly in the soft state and strongly in the hard state (Sakurai et al. 2012; Sakurai et al. 2014; Zhang et al. 2014; Ono et al. 2016).

Since the interpretation of the soft state is rather established (Mitsuda et al. 1984) unlike that of the hard state, to study how the hard state connects to the soft state will reinforce the unified view. The best way for this purpose is to resolve a spectral transition between the two states, and confirm that the spectral parameters in one state connect smoothly and continuously to those in the other state. Although similar attempts have been made (Lin et al. 2007; Church et al. 2014), results remained inconclusive due to the lack of low energy information needed to identify the MCD contribution.

The Suzaku observatory, which has wide band sensitivity covering both the MCD and the Comptonized BB emission, is ideal for the above purpose. Among the Suzaku data of LMXBs, those of Aquila X-1 (hereafter Aql X-1) acquired on 2011 October 21, in particular, have turned out to be the most suited for our purpose, because they caught a hard-to-soft spectral transition in a rising phase of an outburst (Ono et al. 2017). This source is associated with an optical counterpart with a magnitude of $V = 15 - 19$ (Gottwald et al. 1991). The distance has been constrained to be 4.4–5.9 kpc by its type I bursts assuming an NS mass as $M_{\rm NS} = 1.4\ M_\odot$ and the Eddington luminosity at the burst peak (Jonker

& Nelemans 2004). In the present paper, the distance is assumed as 5.2 kpc.

2. Data process

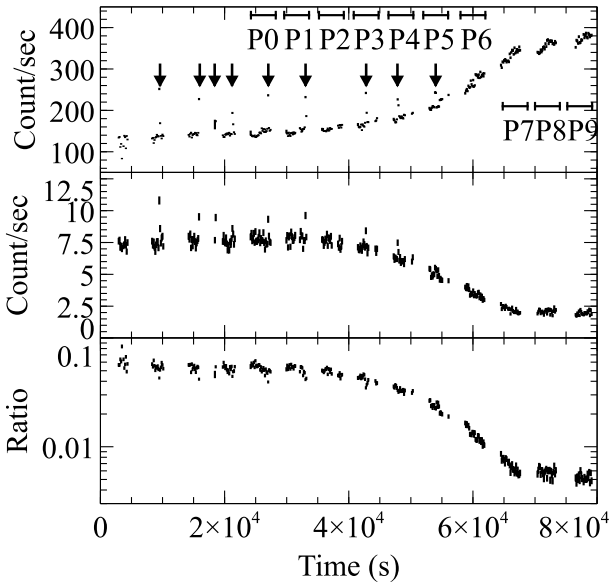

Fig. 1. Background subtracted light curves with 128 s binning of XIS 0+3 in 0.8–10 keV (top) and of dead-time corrected HXD-PIN in 15–60 keV (middle). The bottom panel shows the HXD-PIN vs XIS hardness ratio. The time origin is 2011 October 21 12:51:33. The arrows indicate type I bursts.

We used an archival Suzaku data set of Aql X-1 (ObsID 406010020) acquired from 2011 October 12:51:33 UT for a gross duration of 79.9 ks. The XIS was operated in the 1/4 window mode with a read-out time of 2.0 s. The burst mode option was also employed to accumulate photons for 0.5 s during the 2.0 s read-out time. Details are given in Ono et al. (2017).

XIS 0 and XIS 3 events of GRADE 0,2,3,4 and 6 were used. On-source events were accumulated in a $2'.5$ circle around the image centroid, but excluding events in the innermost $1'$ circle to reduce the pile-up effects (Yamada et al. 2012). Background events were taken from an annular region with the inner radius of $4'$ and the outer radius of $5'$. As shown in fig. 3, we extracted spectra from 10 periods (P0,P1, $\cdots$ P10), but excluding type I bursts.

HXD cleaned events were used as an on-source data after dead time correction. Non X-ray background (NXB) events distributed by the HXD team was subtracted (Fukazawa et al. 2009) from the on-source data. Cosmic-X-ray background (CXB) was accounted for by adding a fixed CXB model to a spectral model. The data were divided in the same way as the XIS.

3. Analysis

As presented in fig. 2, the obtained spectra show a clear transition from P0 to P9. These 10 spectra were all fitted with our unified model (§1), consisting of the MCD plus Comptonized BB emission. XSPEC (version 12.9.0) models `diskbb`, `nthcomp` (Zdziarski et al. 1996; Życki et al. 1999) and `diskline` (Fabian et al. 1989) were used. The seed photons for `nthcomp` were chosen as BB expected to arise from the NS surface. The constructed model, `diskbb+nthcomp+diskline`, was then multiplied with an absorption factor `wabs`, with its column density fixed at 3.6×10^{21} cm^{-1} (Sakurai et al. 2014; Gatuzz et al. 2016). The free parameters are the inner disk radius $R_{\rm in}$, the inner disk temperature $T_{\rm in}$, the BB radius $R_{\rm BB}$, the BB temperature $T_{\rm BB}$, the electron temperature $T_{\rm e}$, the electron optical depth τ, the line centroid energy, the emissivity parameter, and the line normalization. The inner disk radius of `diskline` was tied to $R_{\rm in}$.

All the 10 spectra were reproduced successfully by the model with $\chi^2_\nu < 1.2$ for $298 - 333$ d.o.f. (fig. 2). As shown in fig. 2, the 1–3 keV signal tripled from P0 to P9, which is explained by an increasing MCD flux. The spectrum above ~ 10 keV, in contrast, decreased to about one third, reflecting a decrease in the cutoff energy, and hence in $kT_{\rm e}$.

The obtained parameters are summarized in fig. 3. The inner disk radius was derived using MCD normalization $N_{\rm MCD}$ as

$$R_{\rm in} = \xi \kappa^2 \left(N_{\rm MCD}\right)^{\frac{1}{2}} \left(\frac{D}{10\ {\rm kpc}}\right) (\cos i)^{-\frac{1}{2}}$$

where $D = 5.2$ kpc is the distance, $i = 45^\circ$ is an assumed inclination angle (Sakurai et al. 2012), and $\xi = 0.412$ and $\kappa = 1.7$ are the correction factor of the inner boundary condition and the color-hardening of the disk, respectively (Kubota et al. 1998). The BB radius is calculated assuming photon number conservation in the Comptonization process. In fig. 3a, $R_{\rm BB} < R_{\rm NS} < R_{\rm in}$ is realized throughout, where $R_{\rm NS} = 12$ km is the NS radius, implying a physically reasonable geometry. Through the transition, the three temperatures became closer to one another (fig. 3b). The parameter values in the hard state and those in the soft state are consistent with the typical values found in previous observations of the respective states (e.g. Sakurai et al. 2012, 2014). Most importantly, all the parameters changed continuously and monotonically. Thus, the hard state is smoothly connected to the typical soft state, with reasonable values.

Figure 3c shows the luminosities of the individual physical processes. The disk luminosity $L_{\rm disk}$ was calculated using 0.1–10 keV energy flux of `diskbb` without inclination correction. The BB luminosity $L_{\rm BB}$ was obtained from the `nthcomp` photon flux in 0.1–50 keV and

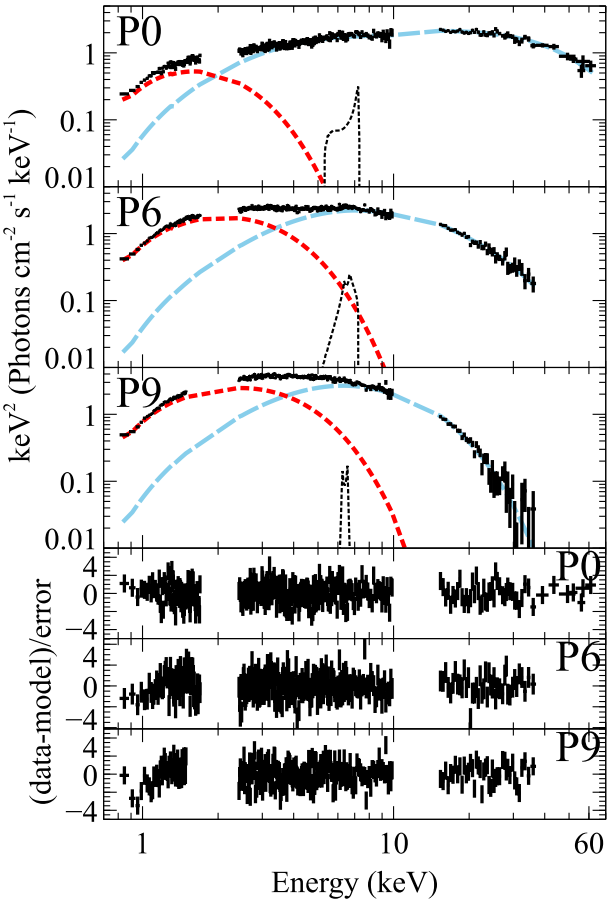

Fig. 2. The Suzaku spectra of Aql X-1 in $\nu F\nu$ form from P0, P6 and P9, acquired with XIS 0+3 (0.8–10 keV), HXD-PIN (15–60 keV) and HXD-GSO (>50 keV). They are fitted with `wabs*(diskbb+nthcomp+diskline)`, and the best fit model is also shown together with its components.

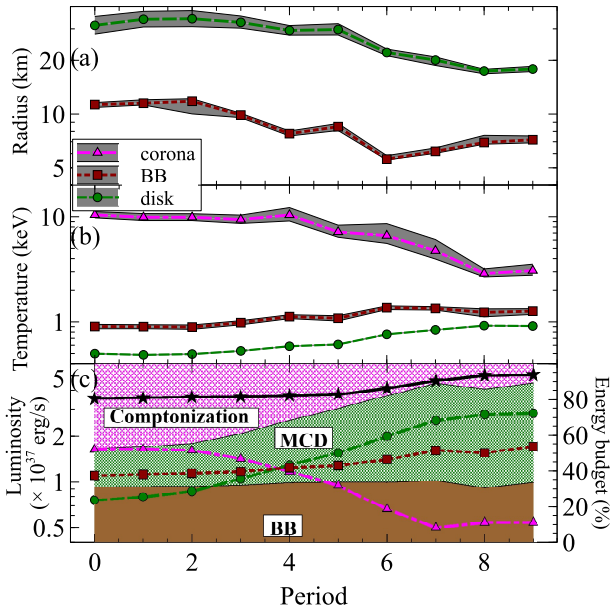

Fig. 3. Evolutions of the spectral parameters obtained from the best fit models, and the luminosities described in §3. Triangles, rectangles and circles represent the corona, BB and the disk, respectively. (a) The radii. (b) The temperatures. (c) The total luminosity (stars), with ordinate on the left. The luminosity fractions of the three processes are also shown with ordinate on the right.

its BB temperature, assuming a photon number conservation and a spherical emission. The Comptonization luminosity $L_{\rm comp}$ was derived by subtracting $L_{\rm BB}$ from the luminosity of the `nthcomp` at 0.1–100 keV. As the total luminosity $L_{\rm t}$ increased in fig. 3c, $L_{\rm comp}$ decreased and $L_{\rm disk}$ increased with a negative correlation. The XIS vs HXD-PIN anti-correlation, first revealed in fig. 1, approximately reflects this $L_{\rm disk}$ vs $L_{\rm comp}$ anti-correlation. The fraction of $L_{\rm BB}$ did not change throughout and is not much different from 50%, which is predicted by the virial theorem (§4.2).

4. Discussion

During the observation of Aql X-1 in its outburst, the transition took place in $\sim$ 30 ks involving a drastic spectral change. Throughout the subdivided 10 periods, the spectra were successfully explained with a common model of `wabs*(diskbb+nthcomp+diskline)`. The obtained parameters evolved continuously and monotonically from the values typical of the hard state to those of the soft state. As a result, the spectral components in the hard state have been firmly identified with those in the soft state.

4.1. Interpretation of the model evolution

As the luminosity increased, the inner disk edge approached the NS surface from $R_{\rm in}$ = 31 km to 18 km. Consequently, $R_{\rm BB}$ decreased from 11 km to 7 km. This suggests that a coronal accretion flow in the hard state is onto the whole NS surface, while that in the soft state become more confined to the NS equator. In association with the above geometrical change, $T_{\rm e}$ decreased due to weaker heating and stronger cooling of the corona. To summarize, the state transition can be interpreted as a transition of the emission from that dominated by a Comptonizing corona to that dominated by an optically thick accretion disk.

4.2. Coronal accretion

In addition to the MCD and BB emission, we can further investigate coronal accretion utilizing the coronal optical depth τ along the line of sight. Here, τ is expressed as

$$\tau = \sigma_{\rm t} \int n_{\rm e} dx \qquad (1)$$

where $\sigma_{\rm t}$ is the Thomson scattering cross section and $n_{\rm e}(R)$ is the electron number density at a radius R. The

mass accretion rate can be expressed as

$$\dot{M} = 1.2 S(R) V_{\rm r}(R) \mu m_{\rm p} n_{\rm e}(R) \quad (2)$$

where 1.2 is the average molecular weight, $S(R) = 4\pi R^2 \zeta$ is the cross section of the corona at R, $0 < \zeta < 1$ is a form factor, $V_{\rm r}(R)$ is the radial velocity at R and $m_{\rm p}$ is the proton mass. We assumed a spherical accretion for simplicity. Using the free-fall velocity $V_{\rm ff} = \sqrt{2GM_{\rm NS}/R}$ where G is the gravitational constant, and a dimensionless parameter g ($0 < g < 1$), we may write as $V_{\rm r} = gV_{\rm ff}(R)$. Substituting $L_{\rm t} = GM_{\rm NS}\dot{M}/R_{\rm NS}$ to eq. (2), $n_{\rm e}$ in eq. (1) can be expressed as $n_{\rm e} = n_{\rm e}(g, R, L_{\rm t})$. Integrating eq. (1) from $R_{\rm NS}$ to $R_{\rm in}$,

$$g\zeta = \frac{0.16}{\tau}\left(\sqrt{\frac{R_{\rm in}}{R_{\rm NS}}} - 1\right)\frac{L_{\rm t}(\ {\rm erg\ s^{-1}})}{10^{37}} \quad (3)$$

is obtained. Substituting the obtained parameter values of τ, $R_{\rm in}$ and $L_{\rm t}$, we derived $g\zeta$ as in fig. 4. The smaller values of $g\zeta$ in the soft state indicate that the scale height of the corona become lower (smaller ζ), and/or the radial coronal velocity is lower (smaller g). In any case, the radial velocity is much smaller than the free fall velocity over the observation, assuming ζ is close to the unity. Therefore, the corona is in fact close to the Keplerian motion.

In order to compare the present results with those from a soft to hard state transition, $g\zeta$ from Sakurai et al. (2015) is also shown in fig. 4. Similarly, i) $g\zeta$ is as small as ~ 0.01 both in the soft and the hard state, and ii) $g\zeta$ is smaller in the soft state than in the hard state, but iii) the change of $g\zeta$ took place at a lower luminosity below $\sim 2 \times 10^{37}$ erg s^{-1} due to the hysteresis. In fig. 4, the source evolve clockwise along the small arrows when the source undergoes an outburst, from the hard state to the soft state, and from the soft state to the hard state.

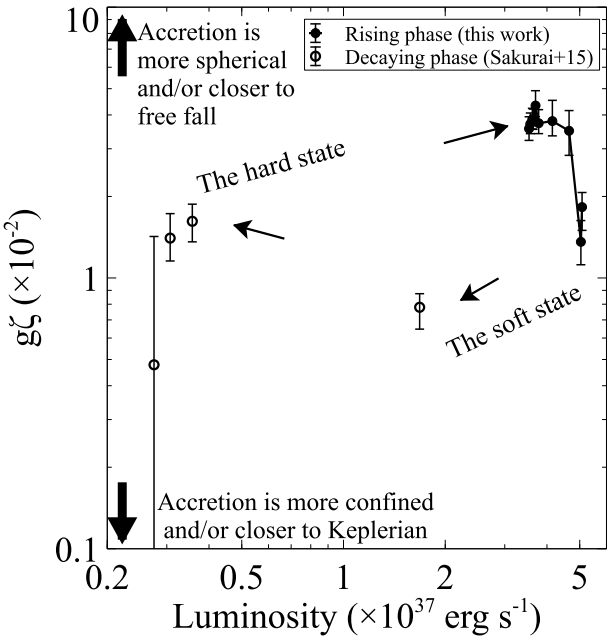

Fig. 4. The evolution of $g\zeta$, from the spectral fit, as a function of $L_{\rm t}$. Filled circles are the present results and the open circles are those taken from Sakurai et al. (2015).

References

Asai, K., Matsuoka, et al. 2012, PASJ, 64,
Fabian, A. C. et al. 1989, MNRAS, 238, 729
Church, M. J. et al. 2014, MNRAS, 438, 2784
Fukazawa, Y., et al. 2009, PASJ, 61, 17
Gatuzz, E., & García, J. A. et al. 2016, A&A, 588, A111
Gottwald, M. & Steinle, H. et al. 1991, A&AS, 89, 367
Jonker, P. G., & Nelemans, G. 2004, MNRAS, 354, 355
Kubota, A., Tanaka, Y. et al. 1998, PASJ, 50, 667
Lin, D., Remillard, R. A. et al. 2007, ApJ, 667, 1073
Mitsuda, K., et al. 1984, PASJ, 36, 741
Ono, K., & Makishima, K. et al. 2016, PASJ, 68, S14
Ono, K., 2017, submitted for publication PASJ
Sakurai, S., Takahashi, H. et al. 2012, PASJ, 64, 72
Sakurai, S., et al. 2014, PASJ, 66, 10
Sakurai, S., 2015, PhD Thesis, The University of Tokyo
Yamada, S., Uchiyama, H., et al. 2012, PASJ, 64, 53
Zhang, Z., & Makishima, K. et al. 2014, PASJ, 66, 120
Zdziarski, A. A. et al. 1996, MNRAS, 283, 193
Życki, P. T., & Done, C. et al. 1999, MNRAS, 309, 561